Mössbauer and EPR Studies of *Azotobacter vinelandii* Ferredoxin I†

Zhengguo Hu,‡ David Jollie,§ Barbara K. Burgess,|| Philip J. Stephens,§ and Eckard Münck*,‡

Department of Chemistry, Carnegie Mellon University, 4400 Fifth Avenue, Pittsburgh, Pennsylvania 15213-3890, Department of Chemistry, University of Southern California, Los Angeles, California 90089-0482, and Department of Molecular Biology and Biochemistry, University of California, Irvine, California 92717

Received July 11, 1994; Revised Manuscript Received September 26, 1994⊗

ABSTRACT: *Azotobacter vinelandii* ferredoxin I (FdI) is a small protein that contains one Fe_4S_4 cluster and one Fe_3S_4 cluster. Previous studies of FdI have shown that the redox potential of the Fe_3S_4 cluster and the MCD and CD spectra of the reduced Fe_3S_4 cluster are pH-dependent. Using Mössbauer and EPR spectroscopy, we have studied FdI in different oxidation states and at different pH values. Here, we report the spin Hamiltonian parameters of the oxidized ($S = {}^1/_2$) Fe_3S_4 cluster at pH 7.4 and the reduced ($S = 2$) Fe_3S_4 cluster at pH 6.0 and 8.5. The pH dependence observed by MCD is also evident in the Mössbauer spectra which show a change of the magnetic hyperfine tensor for one Fe site of the valence-delocalized pair. The Fe_4S_4 cluster is ligated by cysteines 20, 39, 42, and 45, but not by the adjacent cysteine 24. Treatment of FdI with 3 equiv of ferricyanide alters the Fe_4S_4 cluster, yielding a new species, $[Fe_4S_4]'$. The $S = {}^1/_2$ EPR signal of $[Fe_4S_4]'$ has previously been attributed to the formation of a cysteine disulfide radical from Cys24 and cluster sulfide. Here we show that the EPR signal is broadened by ^{57}Fe, indicating that the electronic spin is significantly coupled to the cluster iron. Consistent with this, substantial magnetic hyperfine interactions are observed by Mössbauer spectroscopy. In addition, the average isomer shift of the four Fe sites is smaller for $[Fe_4S_4]'$ than for $[Fe_4S_4]^{2+}$, indicating that the oxidation is iron-based to at least some extent. Incubation of FdI with excess ferricyanide destroys the Fe_4S_4 cluster but leaves the Fe_3S_4 cluster intact. Our studies of (3Fe)FdI show that the $S = {}^1/_2$ spin of the Fe_3S_4 cluster interacts with another paramagnet, presumably a radical generated at the site left vacant by the removal of the Fe_4S_4 cluster.

Azotobacter vinelandii ferredoxin I (FdI)[1] is a small protein, $M_r = 12\,700$, that has been characterized extensively by X-ray crystallography (Stout, 1988, 1989, 1993; Stout et al., 1988; Merritt et al., 1993) and by a variety of spectroscopic methods, among them Mössbauer spectroscopy (Emptage et al., 1980), electron paramagnetic resonance (EPR) (Morgan et al., 1984, 1985; Johnson et al., 1987), circular dichroism (CD), and magnetic circular dichroism (MCD) (Morgan et al., 1984, 1985; Stephens et al., 1985b, 1991; Johnson et al., 1987), and extended X-ray absorption fine structure (EXAFS) (Stephens et al., 1985b). The protein, whose function has not yet been firmly established (Isas et al., 1994), contains two Fe−S clusters separated by ~12 Å (Stout, 1988), an $[Fe_4S_4]^{2+/1+}$ cluster ligated by four cysteines, and an $[Fe_3S_4]^{1+/0}$ cluster coordinated by three cysteines. Both clusters have low reduction potentials: ~−650 mV (*vs* SHE) for the 4Fe cluster and ~−425 mV for the 3Fe cluster (Iismaa et al., 1991; Shen et al., 1993). The potential of the 3Fe cluster is strongly pH-dependent with a pK of 7.8 (Iismaa et al., 1991). In the following, the oxidized $\{[Fe_3S_4]^{1+}, [Fe_4S_4]^{2+}\}$ and one-electron-reduced $\{[Fe_3S_4]^0, [Fe_4S_4]^{2+}\}$ redox states of FdI are designated FdI_{ox} and FdI_{red}, respectively.

The oxidized 3Fe cluster, $[Fe_3S_4]^{1+}$, has a ground state with electronic spin $S = {}^1/_2$ resulting from antiferromagnetic coupling of three high-spin ferric ions (Emptage et al., 1980; Kent et al., 1980). Upon reduction to FdI_{red}, the electron entering the 3Fe cluster is shared equally by a pair of Fe sites, referred to as the delocalized $Fe^{2+}-Fe^{3+}$ pair, while the third Fe site remains high-spin ferric; interactions among the three Fe sites yield a ground state with electronic spin $S = 2$. As shown in the analysis of the Mössbauer spectra of the $[Fe_3S_4]^0$ cluster of *Desulfovibrio gigas* ferredoxin II (Papaefthymiou et al., 1987), understanding of the magnetic properties of the reduced cluster requires consideration of double exchange in addition to the commonly encountered Heisenberg exchange; double exchange, reflecting resonance delocalization, leads to parallel alignment of the spins of the delocalized pair.

Thomson and co-workers (George et al., 1984) have shown that the MCD spectra of the reduced ferredoxin from *Azotobacter chroococcum* are pH-dependent. CD and MCD studies of FdI (Stephens et al., 1991; Johnson et al., 1987) revealed that the reduced $[Fe_3S_4]^0$ cluster exists in two different forms depending on the solution pH, their inter-

† This research was supported in part by National Science Foundation Grant DMB-9096231 (E.M.) and National Institutes of Health Grant GM45209 (B.K.B. and P.J.S.).

* To whom correspondence should be addressed. Fax: (412) 268-1061.

‡ Carnegie Mellon University.

§ University of Southern California.

|| University of California, Irvine.

⊗ Abstract published in *Advance ACS Abstracts,* November 15, 1994.

[1] Abbreviations: FdI, *Azotobacter vinelandii* ferredoxin I; TAPS, 3-[[2-hydroxy-1,1-bis(hydroxymethyl)ethyl]amino]-1-propanesulfonic acid; MES, 4-morpholineethanesulfonic acid.

0006-2960/94/0433-14475$04.50/0

conversion occurring in the pH range 7−8. Detailed MCD studies have shown that the ground-state spin of both cluster forms is $S = 2$. Recent X-ray diffraction studies of FdI_{ox} and FdI_{red} at pH 6.0 and 8.5 have shown that the variation of the pH does not give rise to a major structural change of the Fe_3S_4 cluster or its immediate environment in either redox state (Stout, 1993). Studies of the D15N mutant of FdI (Shen et al., 1993) support the hypothesis that the reduced $[Fe_3S_4]^0$ cluster is protonated at low pH. ^{57}Fe Mössbauer spectroscopy is quite sensitive to the electronic structure of the Fe sites of an Fe−S cluster. In this paper, we compare the zero-field splitting and hyperfine coupling parameters of the $[Fe_3S_4]^0$ cluster at pH 6.0 and 8.5.

Reaction of FdI_{ox} with a large excess of ferricyanide results in the destruction of both Fe−S clusters, yielding apoprotein. However, EPR, CD, and MCD spectroscopies (Morgan et al., 1984, 1985; Stephens et al., 1985b) have identified two intermediates on this pathway. The first intermediate, FDI'_{ox}, is generated by a three-electron oxidation at the site of the Fe_4S_4 cluster without loss of iron. In the second intermediate, termed (3Fe)FdI, the Fe_4S_4 cluster has been selectively removed. FdI'_{ox} exhibits a new $S = {}^1/_2$ EPR signal which arises from the three-electron oxidation at the Fe_4S_4 cluster site. This signal is most easily monitored at ~40−60 K since in this temperature range the $S = {}^1/_2$ EPR spectrum of the $[Fe_3S_4]^{1+}$ cluster is not detectable but the spectrum of the new paramagnetic center, labeled $[Fe_4S_4]'$, remains. MCD studies have shown that the $[Fe_3S_4]^{1+}$ cluster is not affected by the oxidation process. Quite surprisingly, visible/near-UV MCD attributable to the 4Fe cluster is not observed despite the creation of a new paramagnetic species. These observations led to the proposal that the $S = {}^1/_2$ paramagnet is generated by a one-electron oxidation of a cysteine residue coupled with a two-electron oxidation of a cluster sulfide to yield a cysteinyl disulfide radical, Cys-S−S· (Morgan et al., 1984). Recent studies of the C24A mutant of FdI have implicated the nonligating Cys 24 as the cysteine involved in this reaction (Iismaa et al., 1991); according to X-ray crystallography, the S_γ of this noncoordinating residue is only 3.35 Å away from a cluster sulfide (Stout, 1988). In order to illuminate the status of the 4Fe cluster, we have studied samples of FdI'_{ox} exhibiting the "radical" EPR signal using Mössbauer spectroscopy.

Our studies of FdI_{red} and FdI'_{ox} are assisted by simultaneous analysis of FdI_{ox} and (3Fe)FdI_{ox}.

MATERIALS AND METHODS

Cell Growth and Protein Purification. Azotobacter vinelandii cells containing a FdI overexpression plasmid were grown as described previously (Martin et al., 1990; Iismaa et al., 1991) except that ^{57}Fe metal dissolved in a 50:50 mixture of concentrated nitric and hydrochloric acid replaced the normal iron source ($FeCl_3$) in the media and the total iron concentration was reduced to 0.01 mM, i.e., only 10% of that of normal. ^{57}Fe metal (95.7% enriched) was obtained from Advanced Materials Technology. FdI was purified and crystallized as described previously (Stephens et al., 1991).

Reduction of FdI at High and Low pH. Reduction of the Fe_3S_4 cluster at pH 8.5 (0.1 M TAPS buffer) was achieved with $Na_2S_2O_4$ (Stephens et al., 1991) in 10-fold excess over the protein concentration (~2 mM). Due to the pH dependence of the reduction potential of dithionite, reduction of the Fe_3S_4 cluster at pH 6.0 is incomplete even though the reduction potential of the cluster is increased at this pH ($E^{\circ\prime} = -350$ mV). Full reduction of the Fe_3S_4 cluster was accomplished at pH 6.0 (0.1 M MES buffer) using bulk electrolysis at a pyrolytic graphite edge oriented electrode as described previously (Butt et al., 1991) except that tobramycin (10 mM) was used as the redox-inactive promoter.

Ferricyanide Oxidations. Anaerobic oxidations of FdI with potassium ferricyanide (Sigma) were performed as described previously (Morgan et al., 1984; Stephens et al., 1985b) with minor modifications. FdI'_{ox} was produced by adding 3.0 equiv of ferricyanide to the protein (1−2 mM) at 0 °C. The sample was incubated for a time chosen to maximize the intensity of the EPR spectrum of $[Fe_4S_4]'$ (3−6 min, depending on the protein concentration) and then frozen in liquid N_2. Previous studies were performed at protein concentrations of 10−100 μM, at which FdI'_{ox} is formed slowly at room temperature and is stable for several hours. However, at the high protein concentrations required for Mössbauer spectroscopy (>1 mM), the formation and subsequent destruction of FdI'_{ox} occur too fast at room temperature for convenient sample preparation. At 0 °C, the reaction is slowed sufficiently that a homogeneous sample can be obtained. (3Fe)FdI was prepared with 15−20 equiv of potassium ferricyanide as described before (Stephens et al., 1985b). The concentrations of FdI and ferricyanide were determined from the optical absorption at 405 nm (ϵ = 29 800 M^{-1}) and 420 nm (ϵ = 1020 M^{-1}), respectively. Anaerobic conditions were rigorously maintained in a Vacuum Atmospheres glovebox ($O_2 \sim 0.1$ ppm).

EPR spectra were recorded with a Bruker 200D equipped with an Oxford Instruments ESR-9 flow cryostat. Near-IR−visible−near-UV absorption and CD spectra were recorded with a Cary 17 and a Jasco J500C, respectively.

The Mössbauer spectra were recorded with constant acceleration spectrometers using Janis Research, Inc., cryostats that allow variation of temperature from 1.5 to 300 K. One of the dewars houses a superconducting magnet that allows application of magnetic fields up to 8.0 T parallel to the γ-radiation.

Spin Hamiltonian for Analysis of Mössbauer Spectra. We have analyzed the spectra of the $S = 2$ reduced Fe_3S_4 cluster with the spin Hamiltonian:

$$H = D\left[S_z^2 - \frac{1}{3}S(S+1) + \frac{E}{D}(S_x^2 - S_y^2)\right] + \beta\mathbf{H}\cdot\mathbf{g}\cdot\mathbf{S} + \sum_{i=1}^{3}[\mathbf{S}\cdot\mathbf{A}(i)\cdot\mathbf{I}(i) - g_n\beta_n\mathbf{H}\cdot\mathbf{I}(i) + H_Q(i)] \quad (1)$$

where the quadrupole interactions are given by

$$H_Q(i) = \frac{eQV_{\zeta\zeta}(i)}{12}\{3\mathbf{I}_\zeta^2(i) - I(I+1) + \eta(i)[\mathbf{I}_\xi^2(i) - \mathbf{I}_\eta^2(i)]\} \quad (2)$$

The electronic spin S is the cluster spin. D and E are the axial and rhombic zero-field splitting parameters, and $\mathbf{g}$ is the electronic g-tensor. The magnetic hyperfine interactions of the three sites of the Fe_3S_4 cluster are described by the tensors $\mathbf{A}(i)$ where $i = 1, 2, 3$ sums over the three iron sites of the cluster. We have found that the ζ-axes of the electric

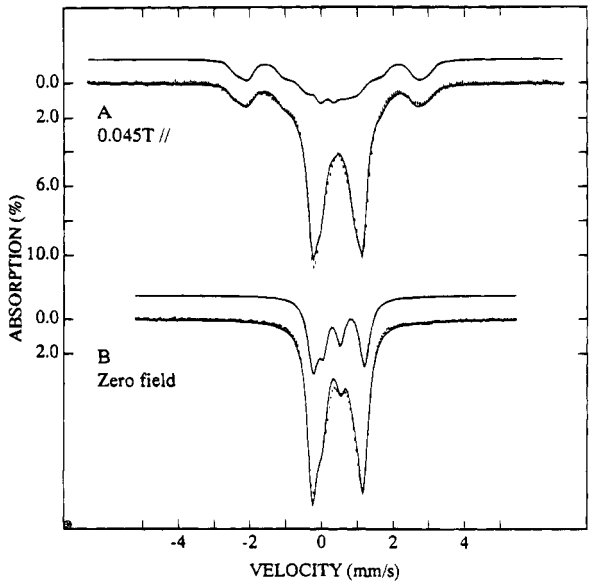

FIGURE 1: Mössbauer spectra of ^{57}Fe-enriched *Azotobacter vinelandii* FdI. (A) Spectrum of FdI_{ox}, pH 7.4, recorded at 4.2 K in a parallel applied field of 0.045 T. The solid curve drawn through the data is a computer simulation describing the seven Fe sites using the parameters of Table 1. The curve drawn above the spectrum indicates the contribution of the $[Fe_3S_4]^{1+}$ cluster. (B) 4.2 K spectrum of FdI_{red}, pH 8.5, recorded in zero field. The solid line through the data is a simulation using the parameters of Table 1. The contribution of the $[Fe_3S_4]^0$ cluster is shown separately as a curve drawn above the data. $[FdI_{ox}]$ was 1.6 mM in 0.1 M phosphate buffer; $[FdI_{red}]$ was 2 mM in 0.1 M TAPS containing 20 mM sodium dithionite.

field gradient tensors (principal axis components $V_{\xi\xi}$, $V_{\eta\eta}$, $V_{\zeta\zeta}$) of the individual sites are rotated relative to the z-axis of the zero-field splitting tensor, and we describe this rotation by the angle β.

Equation 1 is also used for the description of the $S = {}^1/_2$ states of the oxidized $[Fe_3S_4]$ cluster and of the $[Fe_4S_4]'$ species except that the zero-field splitting term is not required. All simulations presented below are based on diagonalizing eq 1 and averaging over the molecular orientations of a frozen solution. We have described the details of such calculations elsewhere (Papaefthymiou et al., 1987).

RESULTS

Reduced FdI. We have studied FdI_{red} at pH 8.5 over the temperature range 1.5−200 K in parallel applied fields up to 8.0 T. Representative spectra, recorded at 4.2 K, are shown in Figure 1B and Figure 2, together with the simulations based on the parameters given in Table 1. As shown previously (Emptage et al., 1980), the electronic ground state of the $[Fe_4S_4]^{2+}$ cluster is diamagnetic. Its contribution to the spectra is illustrated in Figure 2C. Since the spectra of the four sites are slightly different but not resolved, the 4Fe cluster parameters given in Table 1 are not unique. The contributions of the $[Fe_3S_4]^0$ cluster are illustrated in Figures 1B and 2D. The $[Fe_3S_4]^0$ spectra obtained here are quite similar to those of 3Fe clusters from other proteins. The analysis of such spectra has been described in detail (Papaefthymiou et al., 1987; Münck et al., 1993) and is now straightforward. As shown in Figure 1B, the zero-field Mössbauer spectrum of $[Fe_3S_4]^0$ at pH 8.5 consists of two quadrupole doublets. The more intense doublet, representing two nearly equivalent sites, originates

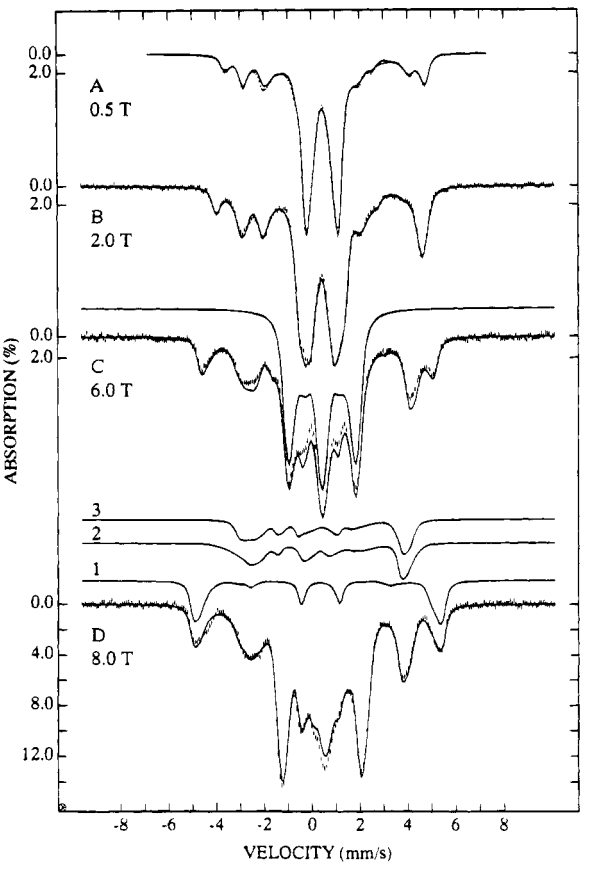

FIGURE 2: Mössbauer spectra of FdI_{red}, pH 8.5, recorded at 4.2 K in parallel applied fields as indicated. The solid lines drawn through the data are spectral simulations based on eq 1 (for the $S = 2$ form of the Fe_3S_4 cluster) using the parameters listed in Table 1. In (C), the contribution of $[Fe_4S_4]^{2+}$ is shown separately. Above the 8.0 T spectrum of (D) are shown spectra of the three subsites of the $[Fe_3S_4]^0$ cluster. [FdI] was 2 mM in 0.1 mM TAPS containing 20 mM sodium dithionite.

from a valence-delocalized $Fe^{3+}-Fe^{2+}$ pair, whereas the third site has parameters characteristic of a valence-trapped Fe^{3+} site. The electronic spins of the three sites are exchange-coupled, by double exchange as well as Heisenberg exchange (Papaefthymiou et al., 1987), to yield a spin $S = 2$ for the ground state of the cluster. Application of a magnetic field polarizes the electronic system and induces magnetic hyperfine interactions. The resultant Mössbauer spectra can be analyzed by means of the spin Hamiltonian of eq 1 with $S = 2$. All reduced 3Fe clusters studied to date have a negative zero-field splitting parameter D of magnitude 2−3 cm^{-1}. This yields a situation where the two lowest levels of the spin quintet are split by $\Delta < 0.5$ cm^{-1}. As a consequence, the magnetic hyperfine interactions are already fully developed in applied fields of only moderate strength, as shown for the 0.5 T data of Figure 2A. [The small value of Δ has allowed the observation of integer spin EPR signals of *D. gigas* FdII at X-band (Münck et al., 1993).] By using the methods described previously (Papaefthymiou et al., 1987), we have determined a parameter set for the reduced $[Fe_3S_4]^0$ cluster that describes the low-temperature spectra for applied fields up to 8.0 T. The theoretical curves shown in Figure 2 were generated using the parameters given in Table 1. As emphasized previously (Papaefthymiou et al., 1987), the low-field ($H < 1$ T) spectra are particularly sensitive to the value of D, and E/D can be determined at

Table 1: Fine Structure and Hyperfine Parameters of Reduced and Oxidized *A. vinelandii* Ferredoxin I; $[Fe_4S_4]^{2+}$ ($S = 0$), $[Fe_3S_4]^0$ ($S = 2$), and $[Fe_3S_4]^{1+}$ ($S = {}^1/_2$)[a]

cluster	ΔE_Q, mm/s	η	β[b]	A_x, MHz	A_y, MHz	A_z, MHz	δ,[c] mm/s	D, cm^{-1}	E/D
$[Fe_4S_4]^{2+}$	1.42[d]	0.8					0.42		
	0.96[d]	0.9					0.43		
$[Fe_3S_4]^0$ (pH 8.5)	−0.47(5)	5(1)		16(1)	14(1)	17.2(2)	0.29	−2.5(5)	0.22(3)
	1.41(5)	1.0	27(5)	−19(1)	−27(2)	−16.7(2)	0.47		
	1.41(5)	0	19(5)	−20(1)	−22(2)	−16.7(2)	0.47		
$[Fe_3S_4]^0$ (pH 6)	−0.47(5)	5(1)		15(1)	14(1)	17.3(2)	0.29	−2.5(5)	0.22(3)
	1.41(5)	−3	20(5)	−21(1)	−25(3)	−14.3(2)	0.47		
	1.41(5)	0.2	24(5)	−19(1)	−22(2)	−16.7(2)	0.47		
$[Fe_3S_4]^{1+}$	+0.63	0.8		−37(1)	−44.7(3)	−44.0(3)	0.30		
	+0.63	1.1		9(3)	21.3(3)	21.8(3)	0.30		
	+0.63	0.2	25	(−9)	(7)	(8)	0.30		

[a] The numbers in parentheses give the estimated uncertainty in the least relevant digits. [b] β rotates the electric field gradient tensor into the principal axis frame of the zero-field splitting tensor. [c] Quoted at 4.2 K vs iron metal at room temperature. [d] This set of parameters provides a good representation of the $[Fe_4S_4]^{2+}$ sites; however, the quoted decomposition is by no means unique.

intermediate fields. Our simulations lead to $\Delta = 0.37 \pm 0.03$ cm^{-1} and $0.19 < E/D < 0.25$. From the relation

$$\Delta = 2D(\sqrt{1 + 3(E/D)^2} - 1) \qquad (3)$$

we then obtain $D = -2.5 \pm 0.5$ cm^{-1}. Figure 2D shows the 8.0 T spectrum together with the theoretical spectra of the three sites of the $[Fe_3S_4]^0$ cluster. Site 1 corresponds to the Fe^{3+} site; this site has a hyperfine tensor with positive components, an expression of the fact that the local spin of the Fe^{3+} site is oriented antiparallel to the system spin $S = 2$. The hyperfine parameters of sites 2 and 3 differ slightly, indicating slightly inequivalent sites for the delocalized pair.

As discussed above, the MCD spectrum of the $[Fe_3S_4]^0$ cluster changes substantially when the pH is lowered to 6.0. In order to further probe the pH dependence of the $[Fe_3S_4]^0$ cluster, we have studied the Mössbauer spectra of FdI_{red} at pH 6.0 over a wide range of applied magnetic fields. Figure 3B compares the 2.0 T spectra of FdI_{red} at pH 6.0 (hash marks) and pH 8.5 (solid circles). By following the movements of the lines of the three sites with increasing applied field, we realized that the differences between the pH 6.0 and 8.5 spectra can be attributed essentially to changes in the parameters of only one site, namely, site 2 of the delocalized pair. (The rightmost line of the site 2 spectrum is marked with an arrow in Figure 3B.) For the lowest electronic level, the expectation value of the electronic spin, $\langle \mathbf{S} \rangle$, is such that $\langle S_z \rangle \gg |\langle S_x \rangle| \gg |\langle S_y \rangle|$. Consequently, the magnetic hyperfine splittings of the Mössbauer spectra are very sensitive to A_z, the component of the magnetic hyperfine tensor along the electronic z-axis. Inspection of the parameters listed in Table 1 shows that A_z of site 2 has changed significantly between pH 6.0 and 8.5. For a reduced $[Fe_3S_4]^0$ cluster, the movement of the Mössbauer absorption lines with increasing applied field depends on H, D, E/D, and the temperature; comparison of the absorption lines of the pH 6.0 and 8.5 samples over the entire range of applied fields suggests that the zero-field splitting parameters are similar at both pH values.

One further observation is noteworthy. Comparison of the 0.5 T spectra of Figure 3A shows that the spectrum of the pH 6.0 sample is less resolved than that obtained at pH 8.5. The unresolved features at pH 6.0 could possibly result from faster spin−lattice relaxation of those molecules of the frozen solution sample for which the applied field is close

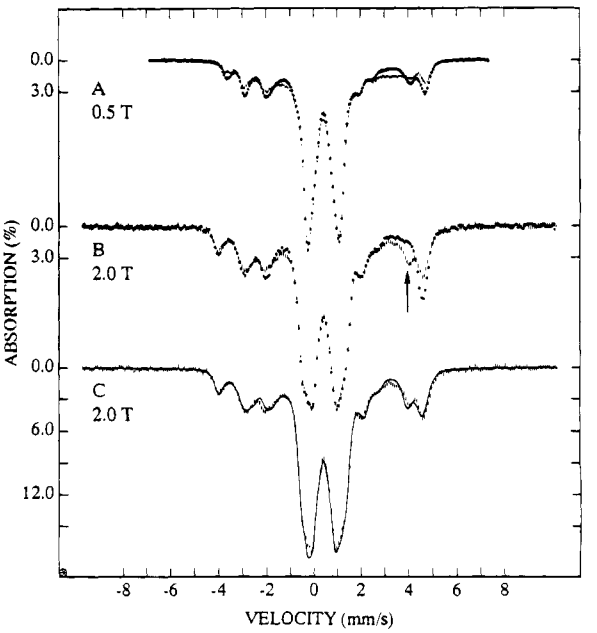

FIGURE 3: Comparison of spectra of FdI_{red} prepared at pH 8.5 (full circles) and pH 6.0 (hash marks). The spectra were recorded at 4.2 K in applied fields as indicated. The arrow in (B) indicates the rightmost line of the spectrum of $[Fe_3S_4]^0$ cluster site 2 as observed at pH 6.0. The solid line in (C) is a spectral simulation of the 2.0 T spectrum of the pH 6.0 sample, generated with the parameters of Table 1. [FdI] was 2 mM in 0.1 M MES buffer containing 0.1 M NaCl and 10 mM tobramycin. FdI was reduced electrochemically as described under Materials and Methods.

to the $x-y$ plane of the zero-field splitting tensor. For the quoted values of D and E, the two lowest levels are separated in energy by less than 0.5 cm^{-1} as long as the applied 0.5 T field is close to the $x-y$ plane. The narrow separation of levels could thus sustain spin−lattice relaxation even at 1.5 K. Alternatively, it is possible that the zero-field splitting parameters have a larger distribution about their mean values at pH 6.0 than at pH 8.5; such heterogeneities tend to broaden the Mössbauer spectra, especially those recorded in weak applied fields.

Oxidized FdI and (3Fe)FdI. Figure 4B−D shows representative Mössbauer spectra of FdI_{ox}. Figure 5A shows the 8K EPR spectrum of the protein used for the Mössbauer study. We have analyzed the low-temperature Mössbauer spectra of the $[Fe_3S_4]^{1+}$ cluster of FdI_{ox} using the spin Hamiltonian of eq 1 with $S = {}^1/_2$. Since such analyses have

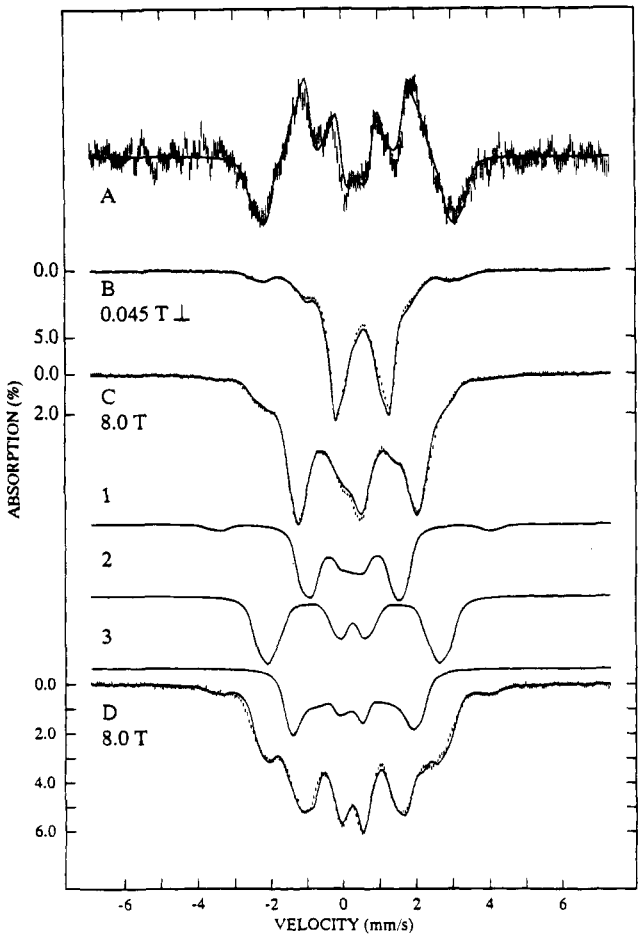

FIGURE 4: Mössbauer spectra of FdI_{ox} and (3Fe)FdI recorded at 4.2 K. (B) Spectrum of FdI_{ox} recorded in a 0.045 T field applied transverse to the observed γ-radiation. (A) Difference spectrum obtained by subtracting the spectrum of (B) from the spectrum of Figure 1A. (C) 8.0 T spectrum of FdI_{ox}. The solid lines in (A)–(C) are theoretical spectra computed with the parameters of Table 1. (D) Mössbauer spectrum of the $[Fe_3S_4]^{1+}$ cluster of (3Fe)FdI recorded in an applied field of 8.0 T. The raw data of this particular sample contained a 15% contribution from $[Fe_4S_4]^{2+}$ that had not been removed by the ferricyanide treatment; this contribution has been subtracted. The solid line drawn through the data is a theoretical curve for the $[Fe_3S_4]^{1+}$ cluster generated from eq 1 with the parameters of Table 1. The curves drawn above the data show the contributions of the individual sites. [FdI_{ox}] and [(3Fe)FdI] were 2 mM in 0.1 M phosphate buffer, pH 7.4.

been described in some detail previously (Kent et al., 1980), we will comment only briefly on some salient spectral features. The spectrum of site 1 is reasonably well resolved from the contributions of the other six Fe sites of FdI, and, therefore, the hyperfine parameters of site 1 can be determined quite reliably. Our data show quite clearly that the magnetic hyperfine tensor of site 1 is anisotropic. Since the local sites of $[Fe_3S_4]^{1+}$ clusters are formally high-spin Fe^{3+}, and since such sites generally exhibit isotropic A-tensors, this result is of considerable interest [see Surerus et al. (1994)]. The spectra of site 2 are substantially masked by the contribution of the $[Fe_4S_4]^{2+}$ cluster. However, its A-tensor can be determined reasonably well by subtracting the spectrum in Figure 4B from the spectrum in Figure 1A; these spectra were recorded at 4.2 K in magnetic fields of 0.045 T applied perpendicular and parallel to the γ-radiation, respectively. Since the spectra of the diamagnetic $[Fe_4S_4]^{2+}$ cluster do not depend on the direction of a weak applied

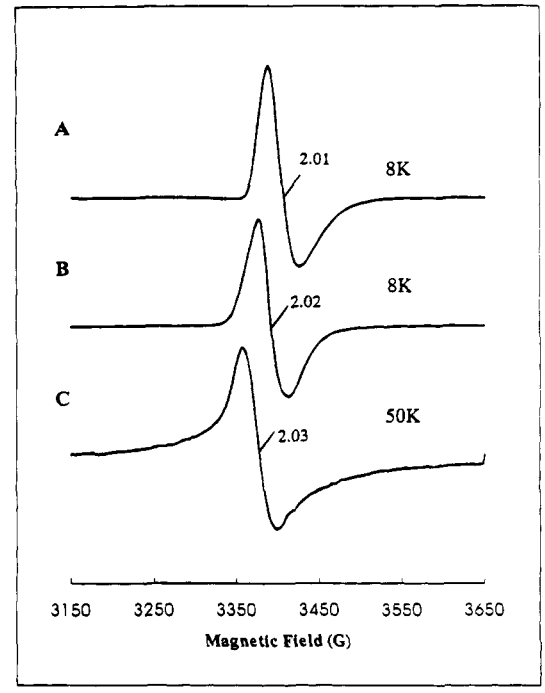

FIGURE 5: X-band EPR spectra of ^{57}Fe-enriched native FdI (A) and (3Fe)FdI (B and C) recorded at the temperatures indicated. Instrumental conditions: all 1 mT modulation amplitude. (A) 20 μW microwave power; 3.2×10^5 gain. (B) 20 μW microwave power; 6.3×10^4 gain. (C) 1 mW microwave power; 3.2×10^5 gain. [FdI] was 0.05 mM in 0.1 M phosphate buffer, pH 7.4; [(3Fe)FdI] was 0.1 mM in the same buffer. Note that $[Fe_3S_4]^{1+}$ does not exhibit an EPR signal at 50 K (Morgan et al., 1984).

field, the resulting difference spectrum, shown in Figure 4A, contains only the contribution of the $[Fe_3S_4]^{1+}$ cluster. Like the A-tensor of site 1, the A-tensor of site 2 exhibits considerable anisotropy. A common feature of all $[Fe_3S_4]^{1+}$ clusters studied to date is the observation of very small A-tensor components for site 3. It has been shown (Kent et al., 1980) that this reflects a spin coupling situation where the local spin of site 3 is oriented nearly perpendicular to the system spin. This site is very difficult to fit for proteins which contain $[Fe_4S_4]^{2+}$ clusters in addition to the $[Fe_3S_4]^{+}$ center, and thus its A-tensor values are substantially less accurately defined.

At temperatures above 30 K, the $S = {}^1/_2$ spin of the $[Fe_3S_4]^{1+}$ cluster relaxes fast on the time scale of Mössbauer spectroscopy; under these conditions, only quadrupole doublets are observed. At 150 K, the spectrum of the FdI $[Fe_3S_4]^{1+}$ cluster consists of only one quadrupole doublet with $\Delta E_Q = 0.63$ mm/s and $\delta = 0.25$ mm/s.

As reported previously (Morgan et al., 1984), appropriate treatment of FdI_{ox} with excess ferricyanide selectively destroys the $[Fe_4S_4]$ cluster, yielding (3Fe)FdI. The 8K EPR spectrum of such a sample is shown in Figure 5B. Comparison of this spectrum with that of FdI_{ox} in Figure 5A shows that the EPR spectrum of (3Fe)FdI is broadened and slightly shifted to lower field. A 150 K Mössbauer spectrum of (3Fe)FdI is shown in Figure 7B. The quadrupole doublet shown is indistinguishable from that of the $[Fe_3S_4]^{1+}$ cluster of the native protein. As observed for other $[Fe_3S_4]^{1+}$ clusters, the three Fe sites display the same isomer shifts and quadrupole splittings. The spectrum also shows the absence of any other iron-containing species; in particular, the Fe_4S_4 cluster has been removed completely by the

ferricyanide treatment.[2] Since the 4Fe cluster is absent, (3Fe)FdI could provide an opportunity for a detailed analysis of the Mössbauer spectra of the Fe_3S_4 cluster. However, the low-field 4.2 K Mössbauer exhibited features suggesting that for a substantial fraction of the molecules the $S = {}^1/_2$ spin of the cluster interacts weakly with another paramagnet. Study of EPR spectra taken at $T = 50$ K (Figure 5C) indeed reveals a previously unrecognized, isotropic signal with intensity corresponding to 0.6−0.8 spin/FdI. It appears likely that a radical exists at the site vacated by the Fe_4S_4 cluster. Analysis of the low-field ($H < 0.5$ T) Mössbauer spectra (not shown) suggests a spin−spin interaction with a coupling strength of $\sim 10^{-2}$ cm^{-1}. This is consistent with dipolar interaction of two spin $S = {}^1/_2$ paramagnets with $g \sim 2$ at 11−13 Å distance. Since an unknown fraction of the molecules exhibit the coupling phenomenon, analysis of the low-field Mössbauer spectra offers no real advantage over the native protein. However, in an applied field of 8.0 T where the spins of the cluster and the radical are decoupled, the spectra can be analyzed without interference by the coupling. Figure 4D shows an 8.0 T spectrum of (3Fe)FdI recorded at 4.2 K. The site 3 *A*-tensor can be reasonably estimated from fits to this spectrum. The solid lines in Figure 4B−D are the result of spectral simulations using the parameters of Table 1. Overall, these parameters fit the data quite well.

FdI′$_{ox}$. FdI′$_{ox}$ is the product of oxidation of FdI$_{ox}$ with 3 equiv of ferricyanide. As discussed above, the Fe_4S_4 cluster is oxidized, yielding a paramagnetic species, $[Fe_4S_4]'$, which exhibits an $S = {}^1/_2$ EPR spectrum but no detectable MCD. The EPR spectrum of the $[Fe_4S_4]'$ center is more easily studied at temperatures above 40 K where the $S = {}^1/_2$ spin of the $[Fe_3S_4]^{1+}$ cluster relaxes rapidly and thus its EPR spectrum does not interfere. Figure 6 shows the 10 K and 50 K EPR spectra of ^{56}Fe- and ^{57}Fe-labeled FdI′$_{ox}$. The spectra of the protein containing ^{57}Fe in natural abundance (2.2%) are identical to those reported previously (Morgan et al., 1984). Labeling FdI′$_{ox}$ with ^{57}Fe substantially broadens the EPR spectrum at both 10 K and 50 K. Since the 50 K spectrum arises from the $[Fe_4S_4]'$ center, it is immediately apparent that the electronic spin of the species is coupled to one or more of the ^{57}Fe nuclear spins. Moreover, FdI′$_{ox}$ samples are homogeneous as judged by the observation that the EPR signal observed at 50 K integrates to nearly 1 spin/mol.

Figures 8 and 9 show Mössbauer spectra of FdI′$_{ox}$ selected from studies in applied magnetic fields up to 8.0 T over the temperature range from 1.5 K to 200 K. Since the spectra are exceedingly complex, it will be useful to the reader that we state some of our major conclusions at the outset.

First, there is no evidence that addition of ferricyanide has any effect on the $[Fe_3S_4]^{1+}$ cluster. This agrees with previous studies which showed that the MCD spectrum of the $[Fe_3S_4]^{1+}$ cluster was unaffected, in shape and amplitude, by the oxidation process (Morgan et al., 1984, 1985). After completion of our studies of FdI′$_{ox}$, the sample was treated with excess dithionite. This treatment eliminated the $[Fe_4S_4]'$ EPR signal and mostly reduced the Fe_3S_4 cluster. Subsequent reoxidation in air restored the Mössbauer spectrum of the $[Fe_3S_4]^{1+}$ cluster to ~43% of the total absorption, i.e., $^3/_7$ of the total Fe of the sample, confirming that the ferricyanide

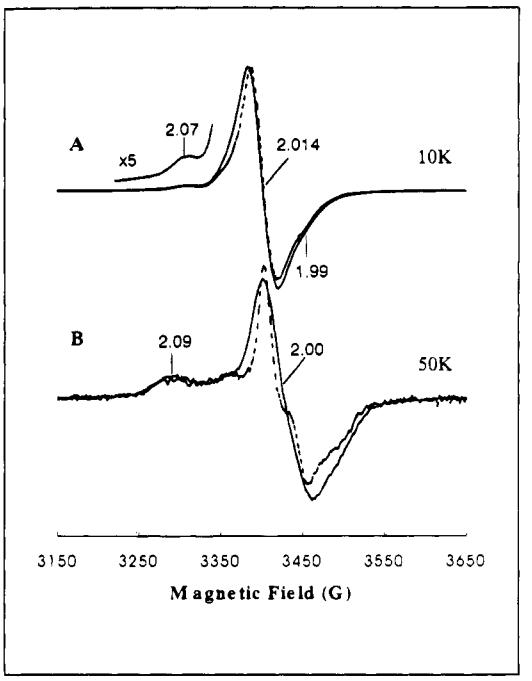

FIGURE 6: X-band EPR spectra of FdI′$_{ox}$ containing ^{57}Fe in natural abundance (dashed lines) and enriched in ^{57}Fe (solid lines). (A) 1 mW microwave power; 6.3×10^3 gain; (B) 1 mW; 10^5 gain; 1 mT modulation amplitude for (A) and (B). [FdI′$_{ox}$] was 0.2 mM in 0.1 M phosphate buffer, pH 7.4.

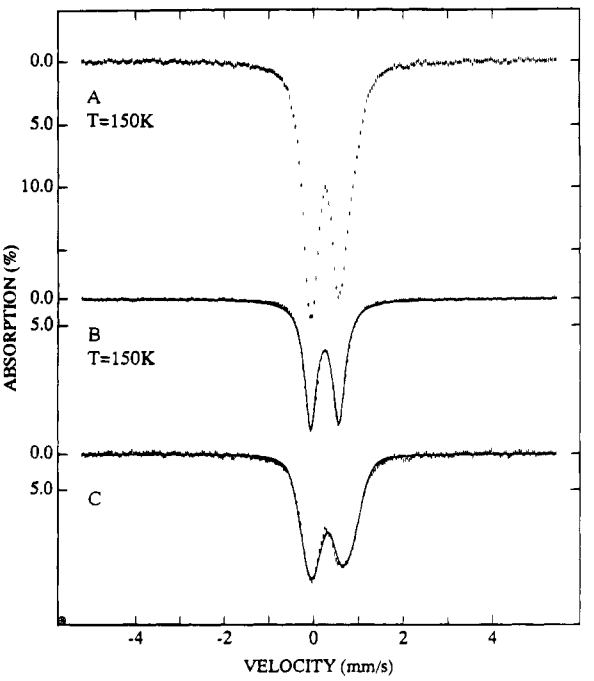

FIGURE 7: Mössbauer spectra of FdI′$_{ox}$ and (3Fe)FdI recorded in zero field at 150 K. (A) Spectrum of FdI′$_{ox}$. (B) Spectrum of (3Fe)-FdI. The solid line in (B) is a least-squares fit to one quadrupole doublet, yielding $\Delta E_Q = 0.63$ mm/s and $\delta = 0.25$ mm/s. (C) Difference spectrum obtained by subtracting the spectrum of the $[Fe_3S_4]^{1+}$ cluster of (B) from the spectrum of (A). The spectrum (C), representing $[Fe_4S_4]'$, was fitted to two quadrupole doublets; parameters are given in the text. [FdI′$_{ox}$] was 2 mM in 0.1 M phosphate buffer, pH 7.4.

[2] We have studied two different (3Fe)FdI samples. The sample of Figure 7B, prepared by adding 20 equiv of ferricyanide, did not contain any discernible contaminant. A second sample, prepared by adding 15 equiv of ferricyanide, contained a 15% Fe_4S_4 contaminant; a spectrum of this sample is shown in Figure 4D.

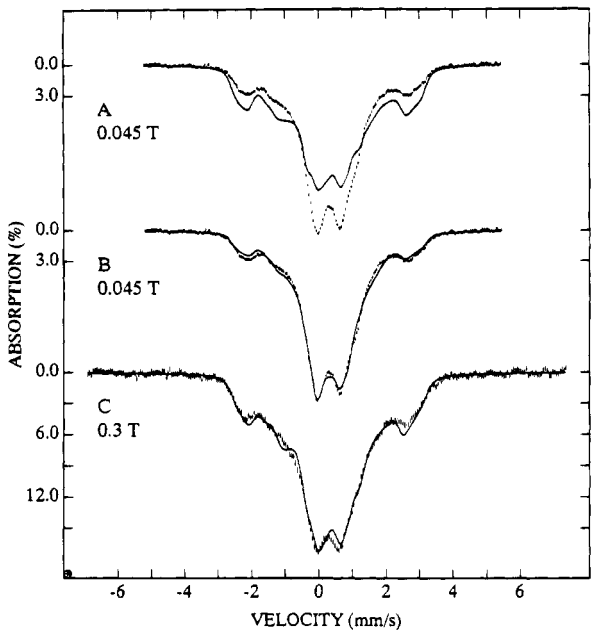

FIGURE 8: Mössbauer spectra of FdI'_{ox} (hash marks) recorded at 4.2 K in a parallel applied field of 45 mT (B) and 0.3 T (C). The solid lines are theoretical curves based on the assumption that the spin $^1/_2$ systems of the $[Fe_3S_4]^{1+}$ cluster and the $[Fe_4S_4]'$ are coupled by a weak exchange interaction. The spin Hamiltonian parameters of both clusters are listed in Tables 1 and 2. The solid line in (A) represents a spectral simulation for the 45 mT data with the same spin Hamiltonian parameters but without consideration of coupling between the clusters. $[FdI'_{ox}]$ was 2 mM in 0.1 M phosphate buffer, pH 7.4.

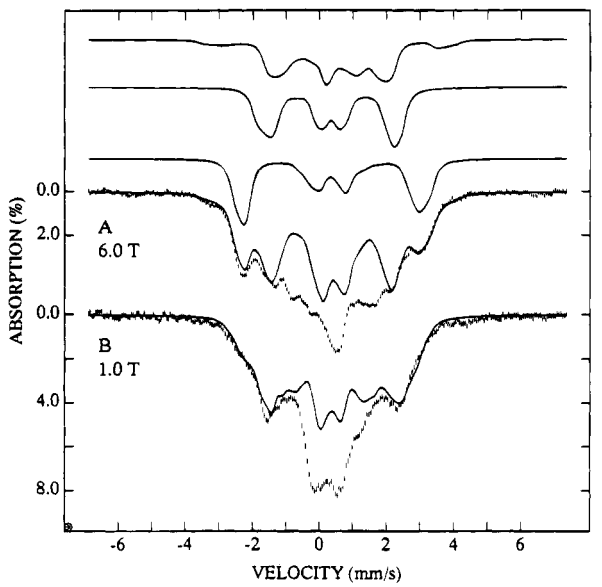

FIGURE 9: Mössbauer spectra of $[Fe_4S_4]'$ obtained at 4.2 K in parallel applied fields of 6.0 T (A) and 1.0 T (B). The spectra were obtained by subtracting the contributions (theoretical spectra) of the $[Fe_3S_4]^{1+}$ cluster from the raw data. The solid lines drawn through the data are spectral simulations to three sites based on an $S = {}^1/_2$ spin Hamiltonian; simulation to the fourth site is not included. Above the 6.0 T data are drawn the theoretical spectra of the individual sites.

oxidation leaves the $[Fe_3S_4]^{1+}$ cluster in a state identical to that observed in FdI_{ox}. The Mössbauer spectra also revealed that ~25% of the Fe of the $[Fe_4S_4]^{2+}$ cluster had been released as Fe^{2+} during the reduction/reoxidation sequence. Apparently some damage occurs when dithionite is added to the ferricyanide-treated sample.

Second, 4.2 K Mössbauer spectra recorded in applied fields ≤0.5 T strongly suggest that the spins of the $[Fe_3S_4]^{1+}$ cluster and of $[Fe_4S_4]'$ interact by spin-dipolar or, perhaps, weak exchange interactions. This is illustrated in Figure 8. Figure 8A (hash marks) shows a Mössbauer spectrum recorded at 4.2 K in an applied field of 45 mT. The solid line in Figure 8B is a theoretical curve computed with the spin Hamiltonian parameters of the $[Fe_3S_4]^{1+}$ cluster (Table 1) and of $[Fe_4S_4]'$ (Table 2), with the additional assumption that the two spin systems interact by an exchange interaction described by ($S_1 = S_2 = {}^1/_2$):

$$H = \mathbf{S}_1 \cdot \mathbf{J} \cdot \mathbf{S}_2 \qquad (4)$$

with $J_{xx} = J_{yy} = 1.5 \times 10^{-3}$ cm^{-1} and $J_{zz} = 2.0 \times 10^{-3}$ cm^{-1}. In Figure 8A, the experimental 45 mT spectrum is compared with a theoretical spectrum generated for $\mathbf{J} = 0$. It is evident that the low-field spectra require consideration of coupling. The presence of spin coupling is, of course, not surprising since the centers of the two Fe−S clusters are only ~12 Å apart in the native protein (Stout, 1988); for this distance, and for $g_1 = g_2 = 2$, the spin-dipolar coupling constant is $g_1 g_2 \beta^2 / \langle r^{-3} \rangle = 1.74 \times 10^{-3}$ cm^{-1}, in good agreement with the above result. The complexity of the situation does not allow us to work out the details of the coupling; the quoted parameters, however, are approximate but of the right magnitude. Most importantly, the above results imply that the two spin systems are essentially decoupled in applied fields $H > 1$ T. (This will permit EPR studies of the uncoupled system at Q-band.)

As a result of this coupling, the EPR spectra of Figure 6A cannot be decomposed into a sum of two *noninteracting* $S = {}^1/_2$ components. Using a computer program that considers two interacting $S = {}^1/_2$ systems, we have attempted to simulate the 10 K EPR spectra. Although inclusion of a coupling term improves the agreement with the data, our attempts have not yet produced a simulated spectrum satisfactory to us. The difficulties encountered in simulating the spectrum of Figure 6A are not surprising for a variety of reasons: (a) Bertrand and co-workers (Guigliarelli et al., 1986) have shown that simulation of the shape of the $g = 2.01$ signal of FdI requires that heterogeneities of the cluster environment (g-strain) be taken into account; (b) the g-values of the $[Fe_4S_4]'$ species are not known with accuracy; and (c) in the case of the ^{57}Fe-labeled sample, the EPR spectrum is broadened by magnetic hyperfine interactions of seven ^{57}Fe nuclei.

We do not yet understand the shapes of the 50 K EPR spectra of Figure 6B either, but we wish to offer the following comments. Owing to fast spin−lattice relaxation, the EPR signal of the $[Fe_3S_4]^{1+}$ cluster of the native protein is unobservable at 50 K [Figure 2A of Morgan et al. (1984)]. Stephens and collaborators have observed that the signal of Figure 6B declines uniformly upon further oxidation of the protein with ferricyanide. It is thus unlikely that the signal observed at 50 K reflects more than one species. Leigh has computed the EPR spectra of a slow-relaxing $S = {}^1/_2$ paramagnet that interacts with a fast-relaxing spin (Leigh, 1970). It is noteworthy that the spectrum of Figure 6B has features similar to those computed by Leigh. If the "Leigh effect" applies here, the $S = {}^1/_2$ spin of the $[Fe_3S_4]^{1+}$ cluster is the fast-relaxing spin that perturbs the spectrum of the paramagnetic $[Fe_4S_4]'$ center.

Table 2: Hyperfine Parameters of the $S = {}^1/_2$ States of the $[Fe_3S_4]^{1+}$ and $[Fe_4S_4]'$ Clusters of *A. vinelandii* FdI, and *C. vinosum* HiPIP $[Fe_4S_4]^{3+}$

clusters	site	ΔE_Q, mm/s	η	A_x, MHz	A_y, MHz	A_z, MHz	A_{av}	δ,[a] mm/s
$[Fe_4S_4]'$	1	−1.01	0	−29	−42	−43	−38	0.42
	2	−0.56	2.0	21	31.5	30.8	27.7	0.34
	3	−0.56	0.9	8	17	19	14.7	0.34
	4	not analyzed						
$[Fe_4S_4]^{3+}$	*a*	−1.03	0.9	−28.2	−30.6	−32.5	−30.4	0.40
C. vinosum HiPIP[b]	*b*	−0.88	0.4	19.2	22.4	19.3	20.3	0.29

[a] Quoted at 4.2 K vs iron metal at room temperature. [b] Quoted from Middleton et al. (1980).

Figure 7A shows a Mössbauer spectrum of FdI'_{ox} recorded at $T = 150$ K. At this temperature, the relaxation rate of both spins is fast on the time scale of Mössbauer spectroscopy (ca. 10 MHz), and both clusters, therefore, exhibit quadrupole doublets. It should be noted that the sample contains no discernible amounts of adventitiously bound Fe^{2+}, nor do the low-temperature EPR and Mössbauer spectra indicate the presence of Fe^{3+}; thus, there is no evidence for cluster destruction. The spectrum of Figure 7C, representing the $[Fe_4S_4]'$ center, was obtained by subtracting the spectrum of the $[Fe_3S_4]^{1+}$ cluster of Figure 7B from the data of Figure 7A, assuming that the $[Fe_3S_4]^{1+}$ cluster contributes ${}^3/_7$ of the total absorption. We have obtained a good fit (solid line) to the spectrum of the $[Fe_4S_4]'$ center by assuming that it can be represented by two quadrupole doublets of equal intensity. The fit shown in Figure 7C yields $\Delta E_Q(1) = 1.01$ mm/s, $\delta(1) = 0.38$ mm/s and $\Delta E_Q(2) = 0.56$ mm/s, $\delta(2) = 0.29$ mm/s. The average shift $\delta_{av} = 0.335$ mm/s is clearly smaller than that of the original $[Fe_4S_4]^{2+}$ cluster, $\delta_{av} = 0.40$ mm/s at 150 K, suggesting that the Fe sites, in particular the two sites with $\delta(2) = 0.29$ mm/s, have lost d-electron density. That the Fe sites of the original $[Fe_4S_4]^{2+}$ cluster have been affected substantially by the three-electron oxidation of the protein is also quite evident from an examination of the low-temperature data.

Figure 9 shows 4.2 K Mössbauer spectra of the $[Fe_4S_4]'$ center, obtained by subtracting the contributions of the $[Fe_3S_4]^{1+}$ cluster from the raw data. It can be seen that the spectra exhibit sizable magnetic hyperfine interactions. In fact, the magnetic splittings of site 1 are larger than those observed for the $S = {}^1/_2$ state of the $[Fe_4S_4]^{3+}$ cluster of oxidized *C. vinosum* HiPIP (see Table 2), showing that the Fe sites of $[Fe_4S_4]'$ experience substantial spin densities. This conclusion is consistent with the observation of broadening of the 50 K EPR spectrum of $[Fe_4S_4]'$ by ^{57}Fe as discussed above.

From studies of the magnetic field dependence of the Mössbauer spectra of $[Fe_4S_4]'$, we have identified the spectra of three subsites. Site 1 has a magnetic hyperfine tensor with negative components and $A_{av}(1) = (A_x + A_y + A_z)/3 = -38$ MHz; the absorption bands of this site move to smaller absolute velocities (toward the center) with increasing applied field. Sites 2 and 3, on the other hand, have *A*-tensors with positive components and smaller magnitudes; $A_{av}(2) = +27$ MHz and $A_{av}(3) = +15$ MHz. Site 4 exhibits small hyperfine interactions, and its absorption is concentrated in the center of the spectra. Considering the lack of resolution and uncertainties in the analysis introduced by subtraction of the spectra of the $[Fe_3S_4]^{1+}$ cluster, we have refrained from analyzing the spectra of site 4.[3]

The spin Hamiltonian parameters of $[Fe_4S_4]'$ are listed in Table 2. It is difficult to estimate meaningful uncertainties for this multiparameter problem. Although we have convinced ourselves that the *A*-tensors are anisotropic, accurate values of these anisotropies are difficult to estimate, especially in view of the unknown asymmetries and orientations of the four electric field gradient tensors. The A_{av} values are currently the best parameters characterizing the sites. It should also be noted that the isotropic nature of the electronic system does not permit correlation of the spatial components of the *A*-tensors and electric field gradient tensors of the three sites for a frozen solution sample; i.e., $A_x(1)$ and $A_x(2)$ do not necessarily refer to the same direction. The reader may ask whether the smaller isomer shifts belong indeed to the sites with the positive *A*-values. It is clear that the doublet of Figure 7C cannot be fitted uniquely to four sites; only $\delta_{av} = 0.335$ mm/s at 150 K is accurately determined experimentally. (We typically find that the second-order Doppler shift increases δ by about 0.05 mm/s when the samples are cooled from 150 K to 4.2 K; this suggests $\delta_{av} = 0.38$ mm/s at 4.2 K.).

DISCUSSION

Previous studies of FdI have shown that the MCD spectra of the reduced $[Fe_3S_4]^0$ cluster are pH-dependent. These studies have also established that the electronic spin of the ground multiplet of the cluster is the same, namely, $S = 2$, at pH 6.0 and 8.5. Recent X-ray crystallographic studies (Stout, 1993) have excluded the possibility that the changes observed by MCD originate from major structural perturbations of the protein structure. Although Asp15, a residue immediately adjacent to the Fe_3S_4 cluster, participates in proton transfer, the pH-dependent MCD change is not linked to protonation, p$K = 7.7$, of this residue; this conclusion is based on the fact that the MCD spectra of the site-directed mutant D15N are identical to those of the native protein (Shen et al., 1993). These observations support the conclusion that the observed pH change involves protonation of the $[Fe_3S_4]^0$ cluster to $[Fe_3S_4]^0$-H^+, presumably at a cluster sulfide.

While MCD spectra of the $[Fe_3S_4]^0$ cluster exhibit major differences throughout the visible and near-UV spectral range upon changing the pH from 6.0 to 8.5, the changes seen by Mössbauer spectroscopy are essentially confined to the magnetic hyperfine tensor of site 2 of the valence-delocalized pair.[4] This observation is consistent with the suggestion that

[3] It is easy to find *A*-values that produce spectra which fill the center of the spectra. Indeed, for our estimate of the coupling, we have included site 4 in the computation of the spectra of Figure 8B,C.

a sulfide becomes protonated at lower pH. We may speculate that this sulfide is not a ligand bridging the two iron sites that form the delocalized pair; if a pair-bridging sulfide were involved, we would expect to see both Fe of the pair similarly affected. The Mössbauer spectra do not indicate significant changes of the zero-field splitting parameters; we found $D = (-2.5 \pm 0.5)$ cm^{-1} at pH 6.0 and 8.5. Analysis of the MCD spectra (Stephens et al., 1991) gave $D = -2.0$ cm^{-1} and $D = -3.5$ cm^{-1} at pH 6.0 and 8.3, respectively. The zero-field splitting analysis of the MCD data assumed $E/D = 0$. Although this disagrees with the results of the present Mössbauer study, namely, $E/D = 0.23 \pm 0.03$ at both pH values, it is unlikely that use of $E/D = 0.23$ would change the results of the MCD analysis in a significant way. Moreover, a comparison of Figures 10 and 13 of Stephens et al. (1991) clearly indicates differences in the raw data obtained at pH 6.0 and 8.3. Possibly, the addition of the glassing agent glycerol for MCD studies could be the cause of some of the differences. On the other hand, the room temperature CD spectra of $[Fe_3S_4]^0$ show a pronounced pH dependence in the absence of the glassing agent, and the Mössbauer spectra of the oxidized Fe_3S_4 cluster were the same in the presence and absence of glycerol. Finally, the results of the two methods are not necessarily in conflict if each method has an uncertainty of ± 0.5 cm^{-1} in the determination of D.

Besides studying the pH dependence of the $[Fe_3S_4]^0$ cluster, we have attempted here to clarify the nature of the $[Fe_4S_4]'$ species by application of Mössbauer spectroscopy. From their EPR and MCD study of $[Fe_4S_4]'$, Morgan et al. (1984) suggested that the three-electron oxidation of FdI_{ox} involves a two-electron oxidation of a cluster sulfide together with a one-electron oxidation of a cysteine residue, leading to a cysteinyl disulfide radical (Cys-S−S•) in the vicinity of a residual diamagnetic Fe_4S_3 core. Recent work (Iismaa et al., 1991) has shown that the participating cysteine is the adjacent Cys24, rather than one of the four cysteine cluster ligands, since ferricyanide oxidation of the C24A mutant did not produce the EPR signal characteristic of FdI'_{ox}. S_γ of Cys24 is extremely close (3.35 Å) to one of the sulfides of the Fe_4S_4 cluster.

The most puzzling aspect of the $[Fe_4S_4]'$ center is the lack of a detectable paramagnetic MCD spectrum. This observation was rationalized (Morgan et al., 1984) by assuming that the cysteinyl disulfide radical is electronically uncoupled from the core of the Fe−S cluster, and as a result, the levels involved in the visible−near-UV spectra of the cluster are not coupled to the electronic spin. The EPR and Mössbauer spectra of the ^{57}Fe-labeled FdI'_{ox} reported here demonstrate that the electronic spin of the $[Fe_4S_4]'$ center is indeed coupled to the ^{57}Fe nuclear spins. Therefore, we now assume that $[Fe_4S_4]'$ is a spin-coupled system consisting of a remnant Fe−S cluster and a radical $S = {}^1/_2$ moiety; the coupling may be by exchange interactions or simply spin-dipolar. Our considerations are hampered somewhat by a lack of knowledge of the spin of the cluster. However, it follows from the oxidation stoichiometry that the electronic spin has to be integer or zero. In evaluating a coupling model, the following EPR and Mössbauer information can be brought to bear on the problem: (a) the g-values are close to $g = 2$ (to within ±5%); (b) the magnitude of the ^{57}Fe magnetic hyperfine interactions is comparable to those of standard $[Fe_4S_4]^{1+}$ and $[Fe_4S_4]^{3+}$ clusters; and (c) the high-field Mössbauer spectra do not indicate any mixing of electronic levels by the applied magnetic field. For cluster spins $S_c = 2$ and *strong* coupling ($J > 5$ cm^{-1}) between the radical and the Fe sites of the cluster [see Münck (1982)], we expect multiplets of half-integer spin with $S \geq {}^3/_2$. Such spin multiplets generally have Kramers doublets with effective g-values equal or larger than $g = 4$, quite distinct from those observed here. As in the strong coupling case, for weak coupling the zero-field splitting parameters (D and E) of the cluster ground multiplet have a pronounced effect on the spectroscopic properties of the system; the ratio $|J|/|D|$ determines the dominant features of the EPR and Mössbauer spectra. We have analyzed for the current and other [see Leising et al. (1991)] problems a variety of coupling schemes. Although the various situations differ in detail, some features are characteristic for many situations. Thus, for $|J| \ll |D|$, the EPR spectra reflect essentially the properties of the radical. As $|J|$ increases, the g-values move away from $g = 2$. Since $g \sim 2$ for $[Fe_4S_4]'$, the EPR data would suggest that $|J| \ll |D|$. For $|J| \ll |D|$, the magnetic hyperfine interactions are proportional to $|J|/|D|$ and therefore small. Since the ^{57}Fe magnetic hyperfine interactions of $[Fe_4S_4]'$ are substantial, the Mössbauer data eliminate the possibility $|J|/|D| \ll 1$. Together with the arguments given above, we can therefore eliminate cluster spins with $S_c = 2$. These considerations suggest a cluster spin $S_c = 1$ or 0.

For the consideration of $S_c = 0$, the electronic model (Münck, 1982) for the coupled chromophores of *Escherichia coli* sulfite reductase can serve as a guide for a discussion; in this enzyme, a high-spin ferric heme is exchange-coupled to an $[Fe_4S_4]^{2+}$ cluster with an $S_c = 0$ ground state (Christner et al., 1981; Cline et al., 1985). For $[Fe_4S_4]'$, we may describe the coupling between the cluster and the presumed radical by

$$H = \sum_{i,j} J_{ij}\mathbf{S}_i\cdot\mathbf{S}_j + \sum_i j_{iR}\mathbf{S}_i\cdot\mathbf{S}_R \qquad (5)$$

where $\mathbf{S}_i$ and $\mathbf{S}_j$ ($i, j = 1,4$; $i < j$) are the spin operators of the Fe sites of the cluster and $\mathbf{S}_R$ is the spin operator of the radical. J_{ij} describes the exchange couplings among the Fe sites, and j_{iR} accounts for the coupling of the radical spin to the ith Fe site. The first sum in eq 5 yields a ladder of cluster spin states with the assumed $S_c = 0$ ground state. For simplicity, we may assume that the radical is coupled effectively to only one Fe site of the cluster, with a coupling constant j_R. For $j_R \ll \Delta$, where Δ is the energy of the lowest

[4] C. D. Stout has recently reported (Stout, 1993) on the basis of X-ray data analysis that the Fe−Fe distances of the Fe_3S_4 cluster of FdI shorten upon reduction at pH 8. This is surprising since the cores of cubane clusters generally expand upon reduction (Berg & Holm, 1982). Moreover, Stout reports that the Fe5−Fe6 distance shortens by 0.11 Å upon reduction to an unprecedented small value of 2.54 Å. Since such a short Fe−Fe distance would promote double exchange (Borshch et al., 1993), the conclusions of the X-ray analysis would suggest that Fe5 and Fe6 form the valence-delocalized pair. However, recent EXAFS studies of the Fe_3S_4 cluster of the ferredoxin from *Pyrococcus furiosus* suggest that the Fe−Fe bond distances are within 2.67 ± 0.01 Å the same in both oxidation states of the cluster (G.N. George, personal communication). Moreover, the Mössbauer spectra of the $[Fe_3S_4]^0$ cluster of both proteins are essentially identical [this work and Srivastava et al. (1993)]. A high-resolution EXAFS study of the $[Fe_3S_4]^0$ cluster of FdI would be desirable. Because reduced (3Fe)FdI lacks the interfering Fe_4S_4 cluster, this protein should be very suitable for such a study.

excited state with $S_c = 1$, the effect of coupling between the cluster and the radical is to mix excited cluster triplet states into the $S_c = 0$ ground state (Münck, 1982). This mixing yields a hyperfine term for the ith Fe site that can be written as $\mathbf{S_R \cdot A_i \cdot I_i}$; here $\mathbf{I_i}$ is the nuclear spin operator of site i and $\mathbf{A_i} \sim (j_R/\Delta)\mathbf{a_i}$ where $\mathbf{a_i}$ is the intrinsic magnetic hyperfine tensor of site i. It can be seen that the magnetic hyperfine interactions of the Fe sites of the cluster become vanishingly small for $|j_R| \ll \Delta$. Clearly, this situation does not apply for $[Fe_4S_4]'$. However, the case $|j_R| \leq \Delta$ is compatible with our data. To date, no Δ-values are available for any 4Fe cluster. However, the diamagnetic ground states of $[Fe_4S_4]^{2+}$ clusters are well separated from low-lying excited states, and we may take $\Delta \geq 100\ cm^{-1}$ as a reasonable estimate. Values of $100\ cm^{-1}$ or larger for j_R imply a superexchange or direct covalent interaction.

For $S_c = 1$, we can readily rule out strong *ferromagnetic* coupling between the radical and the cluster because such coupling would yield a ground state with $S = {}^3/_2$ and thus g-values quite distinct from those observed here. On the other hand, strong *antiferromagnetic* coupling would produce an $S = {}^1/_2$ ground state with properties that might be compatible with our data. For weak coupling, i.e., for $j_R \ll$ zero-field splittings of the presumed $S_c = 1$ multiplet, the magnetic hyperfine interactions would depend on j_R, the zero-field splittings, and the applied field. In weak applied fields, $\beta H \ll |D|$, the ^{57}Fe magnetic hyperfine interactions would be vanishingly small and would saturate for $\beta H > |D|$. Although spin−spin interactions between the $[Fe_4S_4]'$ center and the $[Fe_3S_4]^{1+}$ cluster complicate the data anlysis for data taken in fields <1.0 T, our analysis suggests that the full magnetic hyperfine interactions are already present in the 45 mT spectra; i.e., the Fe sites of $[Fe_4S_4]'$ would exhibit their full internal magnetic fields if the spin−spin interactions with the $[Fe_3S_4]^{1+}$ cluster were absent.

To summarize, the above considerations do not support a model where a radical is *weakly* coupled to a remnant Fe−S cluster. Rather, the coupling must be strong and must involve either a cluster with $S_c = 0$ (the coupling can then be ferromagnetic or antiferromagnetic) or a cluster with $S_c = 1$ antiferromagnetically coupled to the moiety with $S_R = {}^1/_2$. Strong coupling is inconsistent with an isolated cysteinyl disulfide radical.

The facts as we know them at this time regarding the $[Fe_4S_4]'$ center are then as follows: (1) Its visible−near-UV absorption spectrum is very little altered from that of the native $[Fe_4S_4]^{2+}$ cluster. (2) It exhibits an anisotropic $S = {}^1/_2$ EPR spectrum with $g_{av} > 2$ observable at temperatures above 50 K. (3) Its MCD is not detectable in the visible−near-UV spectral region even at temperatures <4 K. (4) The average isomer shift of the four Fe sites is lower than that of the native $[Fe_4S_4]^{2+}$ cluster. (5) At least three of the four iron sites exhibit significant magnetic hyperfine interactions with the paramagnetic center. (6) The presence of cysteine 24 is necessary for the formation of the $[Fe_4S_4]'$ center.

From these data, it is clear that, first of all, the three-electron oxidation to form $[Fe_4S_4]'$ is not *primarily* the oxidation of cluster iron. Oxidation of the Fe−S cluster in which iron oxidation levels change, e.g., $[Fe_4S_4]^{1+} \rightarrow [Fe_4S_4]^{2+} \rightarrow [Fe_4S_4]^{3+}$, is invariably accompanied by a substantial increase in the visible−near-UV absorbance, in contrast to what is observed for $[Fe_4S_4]'$. In addition, while the change in isomer shift indicates some iron oxidation, the changes are approximately half of that observed for the one-electron oxidation of an HiPIP cluster (Middleton et al., 1980). By this measure, less than one-third of the three-electron oxidation taking place is at iron. Since, besides iron, oxidation can only occur at S, either sulfide or cysteine, the conclusion that one or both of these moieties are involved is inescapable. Since the properties of the $[Fe_4S_4]'$ center are inconsistent with those of oxidized HiPIP clusters, a model incorporating a one-electron oxidation at iron (yielding an $[Fe_4S_4]^{3+}$ cluster) together with the two-electron oxidation at S is also unacceptable. We, therefore, continue to be forced to the conclusion that a three-electron oxidation at sulfur sites, i.e., removal of electrons from sulfur-centered orbitals, is the most reasonable zeroth-order description for the formation of $[Fe_4S_4]'$.

The EPR and Mössbauer studies of ^{57}Fe-labeled FdI'_{ox} reported here demonstrate that the cluster iron is not wholly uncoupled from the oxidation reaction; changes in isomer shifts demonstrate some iron oxidation, and the hyperfine coupling parameters demonstrate unpaired electron density at iron. It was argued above that the coupling must be commensurate with intracluster exchange interactions. The description of the $[Fe_4S_4]'$ center is thus not as simple as previously proposed. It is conceivable that the three-electron oxidation leads to the formation of a bond between cysteine 24 and one cluster sulfide, i.e., to an Fe_4S_4 cluster that is ligated by five cysteine ligands.

We are not aware of any structurally characterized Fe−S cluster exhibiting spectroscopic properties similar to those of the $[Fe_4S_4]'$ species. At this time, therefore, it does not appear to be possible to elucidate its geometrical and electronic structures. Some of the unusual properties of $[Fe_4S_4]'$ are not entirely unique, however. The so-called H-cluster of the Fe-hydrogenases (Adams, 1990), which is currently widely thought to be a 6Fe cluster with substantial non-cysteine ligation, exhibits an $S = {}^1/_2$, $g_{av} > 2$ EPR signal in its oxidized state yet exhibits no detectable visible−near-UV MCD originating from an $S = {}^1/_2$ state (Stephens et al., 1985a; Thomson et al., 1985; Zambrano et al., 1989; Rusnak et al., 1987; Wang et al., 1984). The active site of *E. coli* sulfite reductase comprises an Fe_4S_4 cluster covalently linked to a siroheme. The $[Fe_4S_4]^{2+}$ cluster exhibits substantial magnetic hyperfine interactions (Christner et al., 1981) when the siroheme is in a paramagnetic state. This phenomenon has been attributed to an exchange pathway linking one Fe site of the Fe_4S_4 cluster to the paramagnetic siroheme iron (Münck, 1982). The case of the NO derivative of the ferrous siroheme may be particularly relevant. Here, the $S = {}^1/_2$ spin of the NO ligand, thought to be coordinated to the heme on the opposite side from the Fe_4S_4 cluster, gives rise to ^{57}Fe A-values of 20−30 MHz in the $[Fe_4S_4]^{2+}$ cluster (Christner et al., 1983). Clearly, the spectroscopy of all these systems demands further experimental and theoretical attention.

REFERENCES

Adams, M. W. W. (1990) *Biochim. Biophys. Acta 1020*, 115−145.

Berg, J. M., & Holm, R. H. (1982) in *Iron-Sulfur Proteins* (Spiro, T. G., Ed.) pp 1−66, John Wiley and Sons, Inc., New York.

Borshch, S. A., Bominaar, E. L., Blondin, G., & Girerd, J. J. (1993) *J. Am. Chem. Soc. 115*, 5155−5168.

Butt, J. N., Armstrong, F. A., Breton, J., George, S. J., Thomson, A. J., & Hatchikian, E. C. (1991) *J. Am. Chem. Soc. 113*, 6663−6670.

Christner, J. A., Münck, E., Janick, P. A., & Siegel, L. M. (1981) *J. Biol. Chem. 256*, 2098−2101.

Christner, J. A., Münck, E., Janick, P. A., & Siegel, L. M. (1983) *J. Biol. Chem. 258*, 11147−11156.

Cline, J. F., Hoffman, B. M., Mims, W. B., LaHaie, E., Ballou, D. P., & Fee, J. A. (1985) *J. Biol. Chem. 260*, 3251−3254.

Emptage, M. H., Kent, T. A., Huynh, B. H., Rawlings, J., Orme-Johnson, W. H., & Münck, E. (1980) *J. Biol. Chem. 255*, 1793−1796.

George, S. J., Richards, A. J. M., Thomson, A. J., & Yates, M. G. (1984) *Biochem. J. 224*, 247−251.

Guigliarelli, B., More, C., Bertrand, P., & Gayda, J. P. (1986) *J. Chem. Phys. 85*, 2774−2777.

Iismaa, S. E., Vazquez, A. E., Jensen, G. M., Stephens, P. J., Butt, J. N., Armstrong, F. A., & Burgess, B. K. (1991) *J. Biol. Chem. 266*, 21563−21571.

Isas, M. J., & Burgess, B. K. (1994) *J. Biol. Chem. 269*, 19404−19409.

Johnson, M. K., Bennet, D. E., Fee, J. A., & Sweeney, W. V. (1987) *Biochim. Biophys. Acta 911*, 81−94.

Kent, T. A., Huynh, B. H., & Münck, E. (1980) *Proc. Natl. Acad. Sci. U.S.A. 77*, 6574−6576.

Leigh, J. S., Jr. (1970) *J. Chem. Phys. 52*, 2608−2612.

Leising, R. A., Brennan, B. A., Que, L., Jr., Fox, B. G., & Münck, E. (1991) *J. Am. Chem. Soc. 113*, 3988−3990.

Martin, A. E., Burgess, B. K., Stout, C. D., Cash, V. L., Dean, D. R., Jensen, G. M., & Stephens, P. J. (1990) *Proc. Natl. Acad. Sci. U.S.A. 87*, 598−602.

Merritt, E. A., Stout, G. H., Turley, S., Sieker, L. C., Jensen, L. H., & Orme-Johnson, W. H. (1993) *Acta Crystallogr. D49*, 272−281.

Middleton, P., Dickson, D. P. E., Johnson, C. E., & Rush, J. D. (1980) *Eur. J. Biochem. 104*, 289−296.

Morgan, T. V., Stephens, P. J., Devlin, F., Stout, C. D., Melis, K. A., & Burgess, B. K. (1984) *Proc. Natl. Acad. Sci. U.S.A. 81*, 1931−1935.

Morgan, T. V., Stephens, P. J., Devlin, F., Burgess, B. K., & Stout, C. D. (1985) *FEBS Lett. 183*, 206−210.

Münck, E. (1982) in *Iron-Sulfur Proteins* (Spiro, T. G., Ed.) pp 148−175, John Wiley and Sons, Inc., New York.

Münck, E., Surerus, K. K., & Hendrich, M. P. (1993) *Methods Enzymol. 227*, 364−379.

Papaefthymiou, V., Girerd, J.-J., Moura, I., Moura, J. J. G., & Münck, E. (1987) *J. Am. Chem. Soc. 109*, 4703−4710.

Rusnak, F. M., Adams, M. W. W., Mortenson, L. E., & Münck, E. (1987) *J. Biol. Chem. 262*, 38−41.

Shen, B., Martin, L. L., Butt, J. N., Armstrong, F. A., Stout, C. D., Jensen, G. M., Stephens, P. J., LaMar, G. N., Gorst, C. M., & Burgess, B. K. (1993) *J. Biol. Chem. 268*, 25928−25939.

Srivastava, K. K. P., Surerus, K. K., Conover, R. C., Johnson, M. K., Park, J.-B., Adams, M. W. W., & Münck, E. (1993) *Inorg. Chem. 32*, 927−936.

Stephens, P. J., Devlin, F., McKenna, M. C., Morgan, T. V., Czechowski, M., DerVartanian, D. V., Peck, H. D., Jr., & LeGall, J. (1985a) *FEBS Lett. 180*, 24−28.

Stephens, P. J., Morgan, T. V., Devlin, F., Penner-Hahn, J. E., Hodgson, K. O., Scott, R. A., Stout, C. D., & Burgess, B. K. (1985b) *Proc. Natl. Acad. Sci. U.S.A. 82*, 5661−5665.

Stephens, P. J., Jensen, G. M., Devlin, F., Morgan, T. V., Stout, C. D., & Burgess, B. K. (1991) *Biochemistry 30*, 3200−3209.

Stout, C. D. (1988) *J. Biol. Chem. 263*, 9256−9260.

Stout, C. D. (1989) *J. Mol. Biol. 205*, 545−555.

Stout, C. D. (1993) *J. Biol. Chem. 268*, 25920−25927.

Stout, G. H., Turley, S., Sieker, L. C., & Jensen, L. H. (1988) *Proc. Natl. Acad. Sci. U.S.A. 85*, 1020−1022.

Surerus, K. K., Chen, M., Zwaan, J. W., Rusnak, F. M., Kolk, M., Duin, E. C., Albracht, S. P. J., & Münck, E. (1994) *Biochemistry 33*, 4980−4993.

Thomson, A. J., George, S. J., Richards, A. J. M., Robinson, A. E., Grande, H. J., Veeger, C., & Van Dijk, C. (1985) *Biochem. J. 227*, 333−336.

Wang, G., Benecky, M. J., Huynh, B. H., Cline, J. F., Adams, M. W. W., Mortenson, L. E., Hoffman, B. M., & Münck, E. (1984) *J. Biol. Chem. 259*, 14328−14331.

Zambrano, I. C., Kowal, A. T., Mortenson, L. E., Adams, M. W. W., & Johnson, M. K. (1989) *J. Biol. Chem. 264*, 20974−20983.